Research Article

Experimental Study on Liquid Flow and Heat Transfer in Rough Microchannels

Xuan Zhang,[1] Taocheng Zhao,[1] Suchen Wu [iD],[1] and Feng Yao[2]

[1]*Key Laboratory of Energy Thermal Conversion and Control of Ministry of Education, School of Energy and Environment,
  Southeast University, Nanjing 210096, China*
[2]*Jiangsu Key Laboratory of Micro and Nano Heat Fluid Flow Technology and Energy Application,
  School of Environmental Science and Engineering, Suzhou University of Science and Technology, Suzhou, Jiangsu 215009, China*

Correspondence should be addressed to Suchen Wu; scwu2010@seu.edu.cn

Although roughness is negligible for laminar flow through tubes in classic fluid mechanics, the surface roughness may play an important role in microscale fluid flow due to the large ratio of surface area to volume. To further verify the influence of rough surfaces on microscale liquid flow and heat transfer, a performance test system of heat transfer and liquid flow was designed and built, and a series of experimental examinations are conducted, in which the microchannel material is stainless steel and the working medium is methanol. The results indicate that the surface roughness plays a significant role in the process of laminar flow and heat transfer in microchannels. In microchannels with roughness characteristics, the Poiseuille number of liquid laminar flow relies not only on the cross section shape of the rough microchannels but also on the Reynolds number of liquid flow. The Poiseuille number of liquid laminar flow in rough microchannels increases with increasing Reynolds number. In addition, the Nusselt number of liquid laminar heat transfer is related not only to the cross section shape of a rough microchannel but also to the Reynolds number of liquid flow, and the Nusselt number increases with increasing Reynolds number.

1. Introduction

Microscale heat transfer and fluid flow are widely present in micro-electromechanical systems [1], chip laboratories [2, 3], biomedical testing [4], microelectronic chip cooling [5], fuel cells [6], microreactors, and other frontier scientific and technological fields [7, 8]. The research in this field is of great importance at the scientific level for exploring the law of microscale heat and mass transfer. With the rapid development of microfluidic devices, the size of the channel is becoming increasingly smaller, and the ratio of the surface area to the volume of the channel is increasing sharply. As a result, the effect exerted on heat transfer and fluid flow in microchannels by surface roughness is becoming increasingly prominent [9, 10], and the influence mechanism has attracted attention around the world [9, 11]. At present, the role of rough surfaces in microscale heat transfer and flow has not been fully revealed.

The MEMS microchannel heat sink was initially proposed by Tuckerman and Pease [12] in the early 1980s. It possesses the advantages of small size, more area for heat transfer in a limited volume, which contributes to a comparably large heat transfer coefficient. Using microchannel heat sinks has become an important way to deal with the issue of heat dissipation from electronic chips. The microchannel is usually defined as the channel with a size of $10\,\mu m \le D_h \le 200\,\mu m$, in which D_h is the equivalent diameter of the channel [13]. In recent years, scholars in various countries have carried out many theoretical studies on heat transfer and fluid flow in microchannels. Li et al. [14] studied the characteristics of laminar flow and heat transfer in trapezoidal and triangular silicon microchannels in a numerical way and made a comparison with the experimental results. The effect of Reynolds number on Nusselt number was discussed from the view of the field synergy principle. Chen and Zhang et al. quantitatively defined the roughness

structures in microchannels with the fractal theory, which is further expanded by Deng et al. to the construction of porous metal foams [15], and carried out a series of numerical investigations on the effect of relative roughness, the fractal dimension on the heat transfer [16, 17]. Cole and Çetin [18] solved a coupled heat transfer process in parallel-plate microchannels under constant heat flow conditions by means of Green's functions and then obtained analytical solutions in integral form and studied the effect of wall axial heat conduction on liquid flow and heat transfer in microchannels. They also analyzed the influence of flow velocity, length of the heating section, wall thickness, and wall heat coefficient on the average and local Nusselt numbers.

Though the fruitful achievements were obtained based on the theoretical analysis, there have been relatively few reports on experimental results. Kandlikar et al. [19] found that, under the same average roughness conditions, a change in the serrated arrangement of serrated rough surfaces leads to a change in the characteristics of laminar flow in microchannels. This means that the average roughness is not enough to fully reflect the characteristics of rough surfaces, and it is difficult to rely solely on the single index of average roughness to fully explain the influence of roughness on flow characteristics. Kandlikar et al. [20] also measured the effect of surface roughness of stainless-steel small passages with inner diameters of 1.032 mm and 0.62 mm (obtained from acid etching) on the characteristics of flow heat transfer and pressure drop. It was found that the roughness enhanced heat transfer and led to a significant increase in pressure drop. Shen et al. experimentally investigated the single-phase convective heat transfer in a compact heat sink with rectangular microchannels and found that the Reynolds number has a significant effect on the heat transfer capability [21].

In classic fluid mechanics, roughness is nearly negligible for fluid flow in tubes. When the channel size is in microscale, the influence of roughness may permeate into the main flow in the microchannel. In this context, it is expected that the roughness on the surface may play a vital role in microscale fluid flow. To further verify the influence of rough surfaces on microscale liquid flow and heat transfer, the three-dimensional morphology of a stainless-steel surface was observed by scanning electron microscopy, and a performance test system for heat transfer and liquid flow in rough microchannels was designed and built. The variations in the Poiseuille number of liquid laminar flow and Nusselt number of liquid laminar convection heat transfer in rough microchannels with Reynolds number were obtained in this paper.

2. Experimental Description

2.1. Experimental System. The experimental principles of the liquid flow performance measurement in rough microchannels are presented in Figure 1. Methanol was used as the working fluid in the experiments. Driven by injection pumps, the working fluid in syringes flowed through a regulating valve, a constant temperature fluid circulator, a filter, and the experimental section sequentially and finally flowed into glassware (beaker) placed on an electronic

balance. The flow rate of the liquid entering the microchannel was precisely controlled by adjusting the velocity of the liquid pushed by the injection pump, and different flow pressure drop was further obtained. Moreover, the temperature of the liquid entering the microchannel was adjusted by a constant-temperature fluid circulator. The temperature of the liquid inlet in the microchannel was measured by a thermocouple, the pressure drop of the liquid flow in the microchannel was measured by a differential pressure sensor, and the flow rate of the liquid could be set by injection pumps. When the flow rate changed, the flow pressure drop in the microchannel also changed accordingly, which could be obtained by a data acquisition instrument through the differential pressure sensor.

Figure 1 shows that the experimental system for measuring liquid flow performance in rough microchannels is composed of liquid flow control and pressure driving device, experimental section, flow pressure drop testing device, and data acquisition device. The components used in the microscale liquid flow experiments are described in detail as follows.

The liquid flow control and pressure-driving device consists of injection pumps, syringes, and connecting pipes. Two injection pumps with the same size are used in parallel during the experiments, and each of them is equipped with a regulating valve. When one injection pump works, the other injection pump can extract additional working fluid into its syringe over time. Therefore, the continuity and stability of the liquid flow condition can be achieved by switching the injection pumps over time. High-pressure injection pumps are used in the experiments due to the large flow resistance in the microchannels. The inner diameter of the stainless steel syringe is 28.6 mm, and the capacity is 50 mL (see Table 1 for specifications and main parameters), thus ensuring sufficient fluid transport capacity.

The experimental section is mainly composed of rough microchannels and connecting pipes. The rough microchannels are made of stainless steel circular microchannels (Figure 2), which are divided into two types: the inner diameter is 152 μm and 206 μm and the outer diameter is 300 μm and 450 μm, respectively. The average surface roughness heights corresponding to the stainless steel microchannels with inner diameters of 152 μm and 206 μm are 6.65 μm and 6.14 μm, respectively. Channel roughness is generated naturally during microtubule processing. Scanning electron microscopy (SEM) images of the cross sections of the channels and the roughness of the inner surfaces are presented in Figure 3, and the measurements are completed by field emission scanning electron microscopy.

The flow pressure drop test device is composed of a differential pressure sensor and a connecting pipe. Since the range of the pressure drop of the fluid flow in microchannels varies greatly under different working conditions in these experiments, two differential pressure sensors with pressure ranges of 0–200 kPa and 0–500 kPa were selected in the experiments (see Table 1 for specifications and main parameters and Figure 4 for physical photos) to guarantee measurement accuracy, respectively. The connection mode between the differential pressure sensor and microchannel is shown in Figure 5.
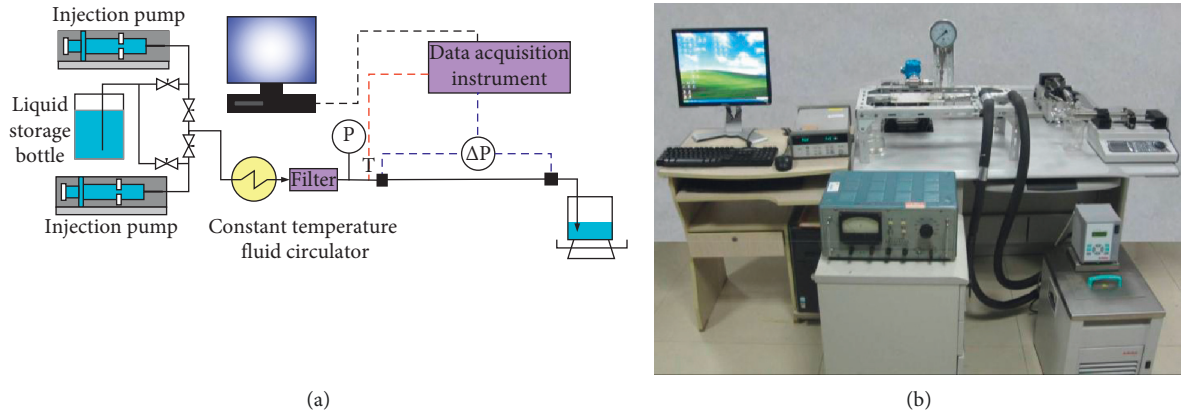
(a)

(b)

FIGURE 1: An experimental system for measuring liquid flow properties in microchannels: (a) schematic diagram and (b) physical photograph.

TABLE 1: Main experimental instruments and equipment and their parameters.

Serial number	Name of instrument and equipment	Specification type, equipment manufacturer, main parameters
1	Single-channel high-pressure injection pump	Model: LSP01-1BH, Baoding Langer Constant Current Pump Co., Ltd. Flow range: 192.7 mL/h~5010.9 mL/h. Flow pushing accuracy: +0.5%. Push pressure: greater than 0.56 MPa
2	Differential pressure sensor	Model: CYR-3D, Shanghai Lingsheng Electronic Instrument co., Ltd. Measurement accuracy: 0.3%, range: 200 kPa and 500 kPa
3	Data acquisition instrument	Model: 34970A, AGILENT Company Scanning rate: 250 channels/s, 3 slots
4	Filter	Model: SS-4F-2, SWAGELOK, USA Size of filter core hole: 0.5 um
5	Thermocouple	Type K, OMEGA Engineering Company, USA The diameter of the thermoelectrode is 0.1 mm.
6	Electric heating rod	Customized
7	Constant temperature fluid circulator	Model: MC, German JULABO company Temperature control range: −35~200 adjustable
8	Voltage regulating transformer	Model: TDGC, 0–250 V adjustable
9	DC regulated power supply	Model: WYJ-45A, Tianjin Radio Component Factory 3 Voltage regulation range: 0~45 V adjustable
10	Field emission scanning electron microscope	Model: ultra plus, ZEISS Germany Resolution: 1 nm @ 15 kV; acceleration voltage: 0.02 kV to 30 kV

FIGURE 2: Stainless steel circular microchannels.

The data acquisition device is composed of a data acquisition instrument, data acquisition module, and computer. The signal lines of a temperature sensor and pressure sensor are connected to the data acquisition module, which is inserted into the module slot of the data acquisition device. An Agilent 34970A data acquisition instrument and Agilent 34901A data acquisition module produced by Agilent Company were used in the experiments. The data acquisition instrument is equipped with Agilent Benchlink Data Logger
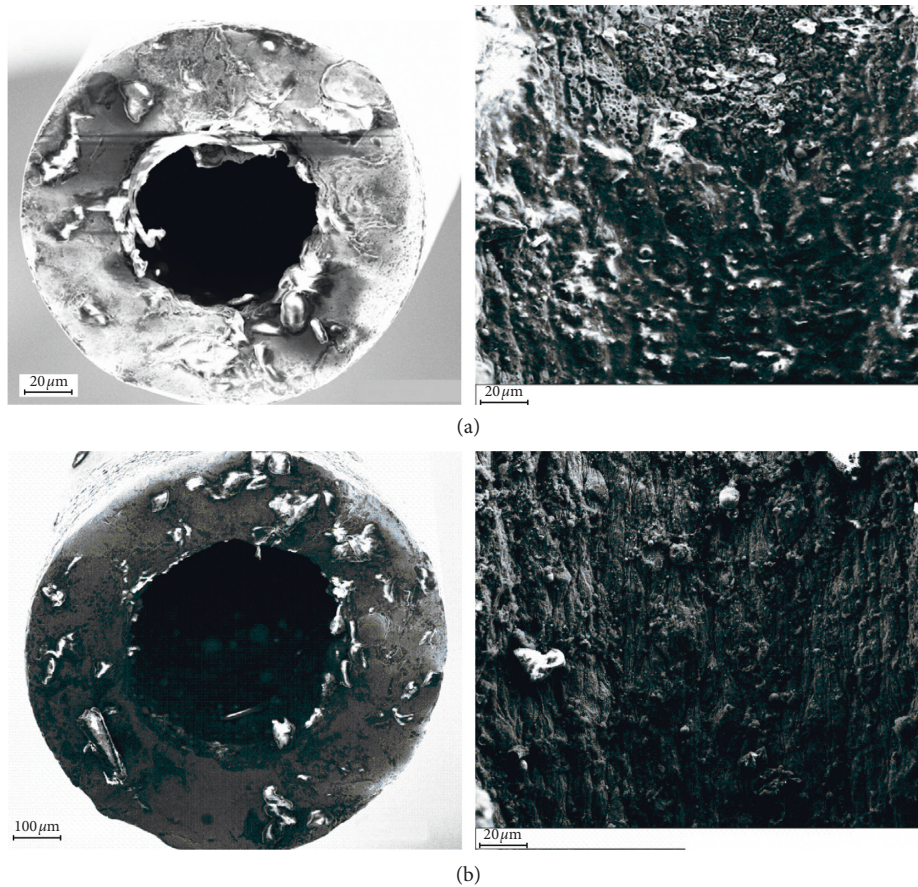
(a)

(b)

FIGURE 3: Physical images of the cross sections and rough surfaces of microchannels: (a) $d = 152 \, \mu$m; (b) $d = 206 \, \mu$m.
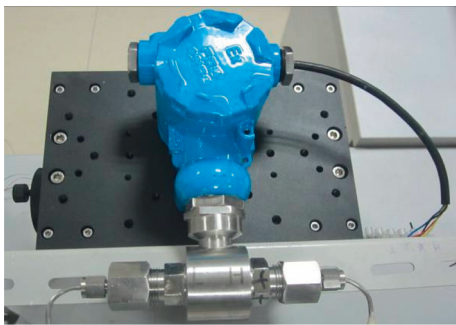

FIGURE 4: Differential pressure sensor (type: CYR-3D).

data acquisition software, which can record, collect, display, and save the measured data in real time on the computer.

On the basis of the abovementioned experimental platform for liquid flow in rough microchannels (Figure 1), experimental research on the liquid convection heat transfer characteristics in rough microchannels can be carried out by just adding a heat source to the experimental section and assisting the measurement of wall temperature of microchannel heat exchanger tubes. Figure 6 shows the experimental section in the experiment of examining the convection heat transfer, which consists of an upper cover plate, a microchannel heat exchanger tube, a heat-conducting block,

an electric heating rod, and a lower cover plate. The upper cover plate, the heat-conducting block, and the lower cover plate are all made of aluminum plates by a milling machine. A rough microchannel of the stainless steel tube with the same specifications as in the microflow experiments is adopted in the microchannel heat exchanger tube.

The electric heating rod is used to simulate the heating element, and the heat generated by it is transferred to the microchannel heat exchanger via the heat-conducting block. The heat in the microchannel heat exchanger is carried away by the convective heat transfer of the working fluid methanol. The thermal insulation material is wrapped on the outer surface of the experimental section to realize the thermal insulation of the experimental section. According to the principle of heat balance, the heat carried by the liquid working medium is transferred to the microchannel heat exchanger by the electric rod. The wall temperature along the microchannel is measured by a thermocouple. Five thermocouples are arranged on the wall of the rough microchannel heat exchanger tube, and the thermocouple wires are drawn to the data acquisition instrument through small round holes in the upper cover plate.

The electric heating rod is connected to a DC-regulated power supply, and the heating power generated by the heating rod is controlled by changing the DC-regulated power supply to regulate the heating flux on the surface of
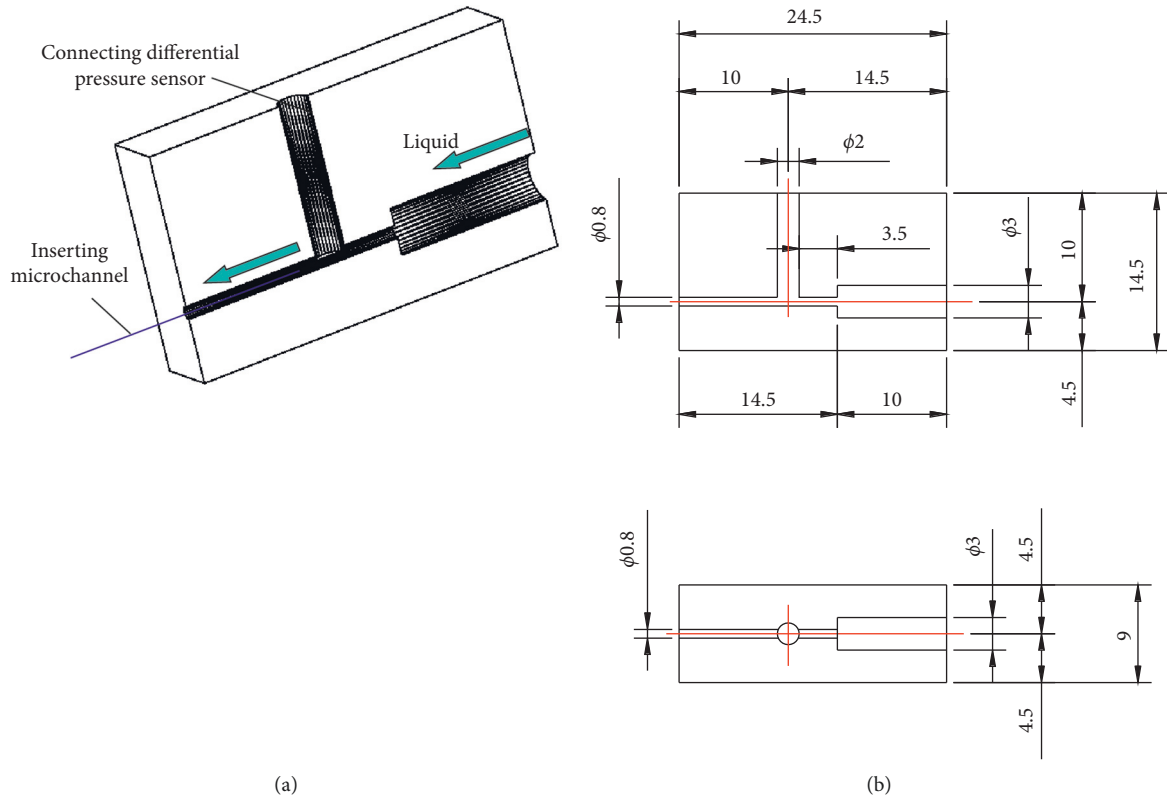
(a)

(b)

FIGURE 5: Connection between the differential pressure sensor and microchannel: (a) schematic diagram; (b) size of the connection structure (unit: mm).
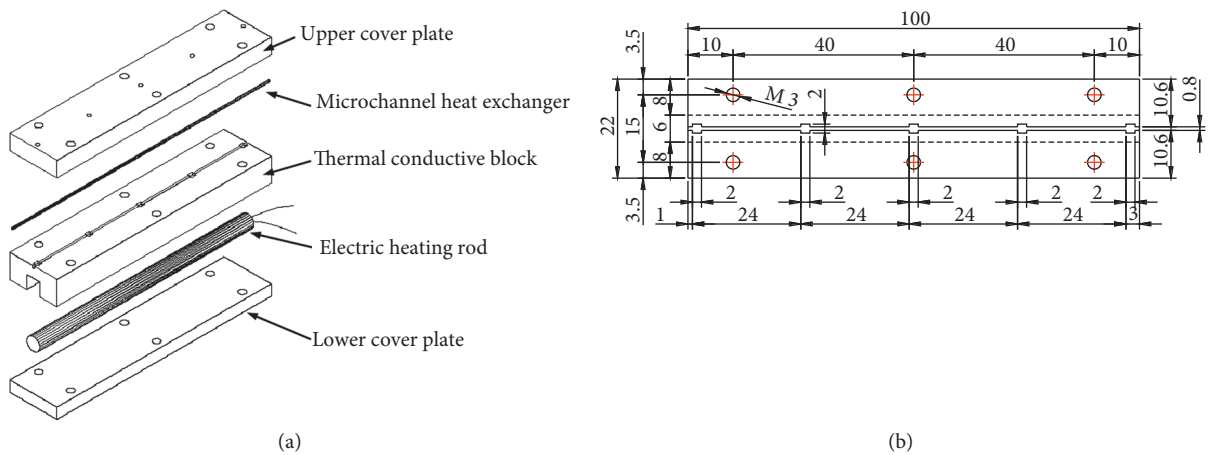

(a)

(b)

FIGURE 6: Schematic diagram of the heat transfer and liquid flow test sections in a microchannel: (a) schematic diagram; (b) structure size of heat-conducting block.

the microchannel. By setting the flow rate of the injection pump to adjust the flow rate of liquid in the microchannel, the experimental conditions of heat transfer and flow in the microchannel under different Reynolds numbers were obtained, and the temperature of the liquid entering the microchannels was adjusted by a constant-temperature fluid circulator.

2.2. Experimental Data and Error Analysis

2.2.1. Fluid Flow.
The Poiseuille number (Po = fRe) is used to evaluate the flow resistance characteristics of the working fluid in microchannels with roughness in this paper, and the flow frictional resistance coefficient f is defined as follows [22]:

$$f = \Delta P \cdot \frac{d}{L} \cdot \frac{1}{2\rho_l \overline{u}_l{}^2}, \tag{1}$$

where ΔP is the on-way resistance of liquid flow in rough microchannels, d represents the diameter of circular microchannels, L symbolizes the length of channels, and ρ_l is the density of the liquid. The average velocity of the liquid flowing through the cross section of the microchannel $\overline{u}_l$ is

$$\overline{u}_l = \frac{G_l}{A} = \frac{4G_l}{\pi d^2}, \tag{2}$$

where G_l is the volume flow rate of liquid and A is the cross-sectional area of the channel. The Reynolds number of liquid methanol flowing in microchannels can be expressed as follows:

$$\mathrm{Re} = \frac{\overline{u}_l d \rho_l}{\mu_l} = \frac{4G_l \rho_l}{\pi \, d \mu_l}, \tag{3}$$

where the dynamic viscosity of the liquid is μ_l. The Poiseuille number of liquid flowing in the microchannel can be obtained by simultaneously solving equations (1) and (3) as follows:

$$\mathrm{Po} = f\mathrm{Re} = \frac{2\pi \Delta P d^4}{L G_l \mu_l}. \tag{4}$$

2.2.2. Heat Transfer.
The average convective heat transfer coefficient of methanol flowing in stainless steel microchannels with inner diameter d and length L is

$$\overline{h} = \frac{Q}{A\left(\overline{T}_w - \overline{T}_l\right)}, \tag{5}$$

where the heat Q transferred from the heat source to the working fluid through the wall of the microchannel is the heat carried away by the working fluid, i.e.,

$$Q = G_l \rho_l C_{p,l}\left(T_{\mathrm{out},l} - T_{\mathrm{in},l}\right). \tag{6}$$

The total heat transfer area of the microchannel heat exchanger tube is

$$A = \pi \mathrm{d} L, \tag{7}$$

and the average temperature of the liquid working fluid is

$$\overline{T}_l = \frac{T_{\mathrm{in},l} + T_{\mathrm{out},l}}{2}. \tag{8}$$

The average wall temperature of the channel is

$$\overline{T}_w = \frac{T_{w,1} + T_{w,2} + T_{w,3} + T_{w,4} + T_{w,5}}{5}. \tag{9}$$

The average Nusselt number of heat transfer and liquid flow in the microchannel can be obtained by simultaneously solving equations (5)~(9) as

$$\overline{\mathrm{Nu}} = \frac{\overline{h}d}{\lambda_l} = \frac{Q}{A\left(\overline{T}_w - \overline{T}_l\right)} \frac{d}{\lambda_l}$$

$$= \frac{G_l \rho_l C_{p,l}\left(T_{\mathrm{out},l} - T_{\mathrm{in},l}\right)}{\pi \lambda_l L\left(\left(T_{w,1} + T_{w,2} + T_{w,3} + T_{w,4} + T_{w,5}/5\right) - \left(T_{\mathrm{in},l} + T_{\mathrm{out},l}/2\right)\right)}, \tag{10}$$

where $C_{p,l}$ is the specific heat capacity of the liquid; $T_{\mathrm{out},l}$ and $T_{\mathrm{in},l}$ are the inlet and outlet temperatures of the liquid in the microchannel, respectively. $T_{w,1}$, $T_{w,2}$, $T_{w,3}$, $T_{w,4}$, and $T_{w,5}$ are the measured surface temperatures along the wall of the microchannel; G_l is the volume flow of liquid through the heat exchanger tubes; and λ_l is the thermal conductivity of the liquid. It should be pointed out that the average temperature of the liquid at the inlet and outlet is taken as the qualitative temperature for the physical parameters of the liquid involved in the above formula.

2.3. Error Analysis.
The indirectly measured y and multiple independent directly measured $x_1, x_2, \ldots$, have the following functional relationship,

$$y = f\left(x_1, x_2, x_3, \ldots, x_n\right). \tag{11}$$

The standard errors of $x_1, x_2, \ldots,$ are $\delta x_1, \delta x_2, \ldots,$ respectively, and then the standard errors of y can be obtained by the following formula [23]:

$$\delta y = \sqrt{\left(\frac{\partial f}{\partial x_1} \delta x_1\right)^2 + \left(\frac{\partial f}{\partial x_2} \delta x_2\right)^2 + \cdots + \left(\frac{\partial f}{\partial x_n} \delta x_n\right)^2}, \tag{12}$$

where the error transfer coefficient is $\partial f / \partial x$. According to formulas (4), (10), and (12), the uncertainty of the Poiseuille number and Nusselt number can be deduced as follows, respectively:

$$\frac{\delta \mathrm{Po}}{\mathrm{Po}} = \pm \left[\left(4\frac{\delta d}{d}\right)^2 + \left(\frac{\delta G_l}{G_l}\right)^2 + \left(\frac{\delta \mu_l}{\mu_l}\right)^2 + \left(\frac{\delta \Delta P/L}{\Delta P/L}\right)^2\right]^{1/2},$$

$$\frac{\delta \overline{\mathrm{Nu}}}{\overline{\mathrm{Nu}}} = \pm \left[\left(\frac{\delta Q/A}{Q/A}\right)^2 + \left(\frac{\delta d}{d}\right)^2 + \left(\frac{\delta \lambda_l}{\lambda_l}\right)^2 + \left(\frac{\delta \left(\overline{T}_w - \overline{T}_l\right)}{\overline{T}_w - \overline{T}_l}\right)^2\right]^{1/2}. \tag{13}$$

The measurement errors of the main parameters involved in these experiments are listed in Table 2.

Before conducting the fluid flow and heat transfer experiments on such a performance test system, a validation examination on this system with a conventional circular channel was launched, in which the diameter of the channels is 3 mm. The pressure drop and the temperature distribution of the liquid laminar flow in this smooth channel are experimentally examined. The Poiseuille number and Nusselt number in the experiment are evaluated as 16.7 and 4.3 when Reynolds number is $1000 < \mathrm{Re} < 2000$, which are consistent with the classic values of $\mathrm{Po} = 16.0$, $\mathrm{Nu} = 4.36$ for

TABLE 2: List of experimental errors.

Parameter	Uncertainty	Parameter	Uncertainty
G_l	0.5%	λ_l	0.02%
ρ_l	0.07%	μ_l	0.6%
L	1.4%	$\overline{T_w} - \overline{T_l}$	2.5%
d	1.7%	Q/A	2.4%
ΔP	0.3%	$\Delta P/L$	1.5%
Po	7.0%	$\overline{Nu}$	3.9%

liquid laminar flow in conventional circular channels, verifying the validity of this experimental approach [24, 25].

3. Results and Discussion

3.1. Fluid Flow in Rough Microchannels. Based on the experimental system shown in Figure 1, the flow pressure drop in rough stainless microchannels with diameters of $152\,\mu m$ and $206\,\mu m$ and length of 7.2 cm was examined. Figure 7 demonstrates the variation of pressure drop with volume flow, and it is observed that the flow pressure drop increases with increasing liquid flow rate. Under the condition of the same flow rate, a decrease in channel diameter leads to rapid growth in the flow pressure drop along the microchannel. The flow pressure drop along the $152\,\mu m$ microchannel is approximately 3.5 times that of the $206\,\mu m$ microchannel.

The variation in the Poiseuille number of liquid flow in microchannels with Reynolds numbers measured by experiments is displayed in Figure 8. Note that the dash-dot line in the figure is the classic value of Poiseuille number for liquid laminar flow in conventional size channels. Generally, for fluid flow in conventional channels, Poiseuille number is just dependent on the shape of the cross section of the channel according to the theory of classical fluid mechanics [24, 25]. However, it is seen in Figure 8 that the Poiseuille number of liquid laminar flow in rough microchannels relies not only on the shape of the cross section of the channel but also on the Reynolds number of the liquid flow. With an increase in the Reynolds number, the roughness results in an increase in the Poiseuille number of liquid laminar flow in the microchannels, indicating that the laminar flow characteristics in rough microchannels differ from those in conventional microchannels.

In roughness microchannels, the uneven surface distribution disturbs the laminar flow near the wall surface and even contributes to the occurrence of eddies in the concave of these rough structures. Since the size of the rough structure (~1 mm) is comparable to the diameter of the roughness microchannel (~100 mm), these induced eddies would inevitably result in the increase of on-way flow resistance. As a result, the Poiseuille number of the laminar flow in roughness microchannels gets elevated when compared with that obtained in conventional channels. Besides, the effect of eddies on the mainstream flow becomes more significant with the increase of Reynolds number, and thus the Poiseuille number gets more deviated from the classic value.
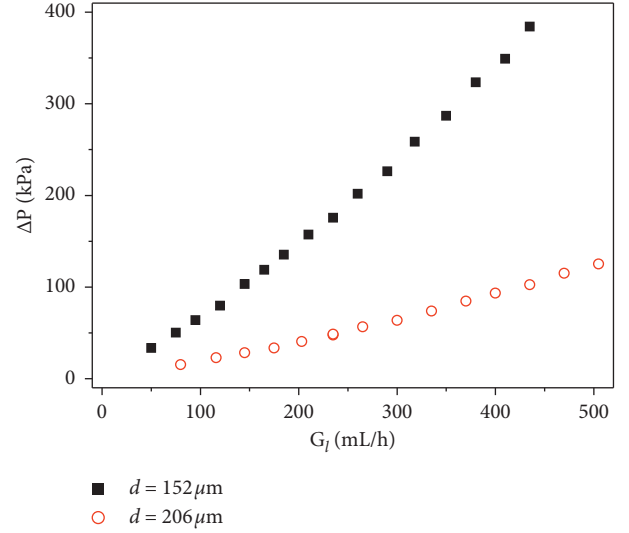

FIGURE 7: Pressure drop of liquid flow in microchannels at different flow rates ($T = 40°C$, $L = 7.2$ cm).
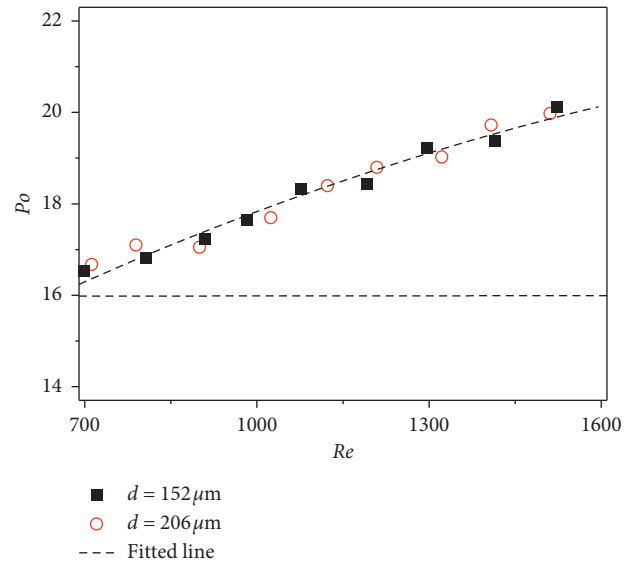

FIGURE 8: Influence of the Reynolds number on the Poiseuille number of liquid flow in microchannels.

In addition, to clearly reveal the relationship of Reynolds number and Poiseuille number in the circular roughness microchannel, following the work of Wu and Cheng [26], a correlation equation with the consideration of the relative roughness is proposed as $Po = C_1 \varepsilon^{a_1} Re^{b_1}$, in which ε is the relative surface roughness of the microchannel. Based on the obtained experimental data, the parameters in the equation are fitted as $C_1 = 3.04$, $a_1 = -0.001$, and $b_1 = 0.256$. The correlation equation is also plotted in Figure 8, and it is seen that it well predicts the relationship between Poiseuille number and Reynolds number.

3.2. Heat Transfer in Rough Microchannels. The variation in the wall temperature along the flow direction of the
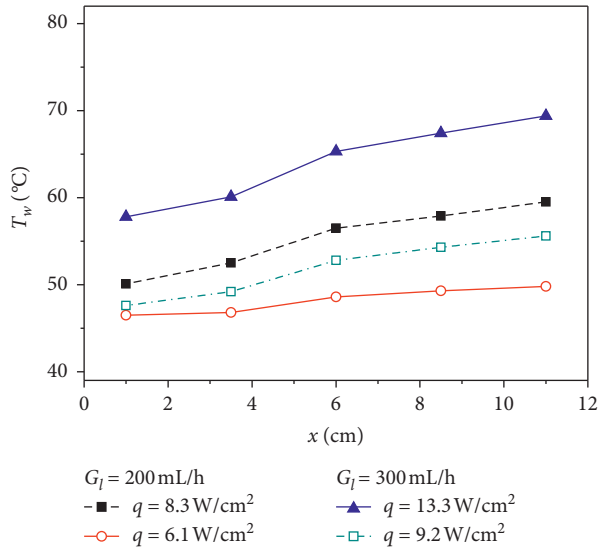
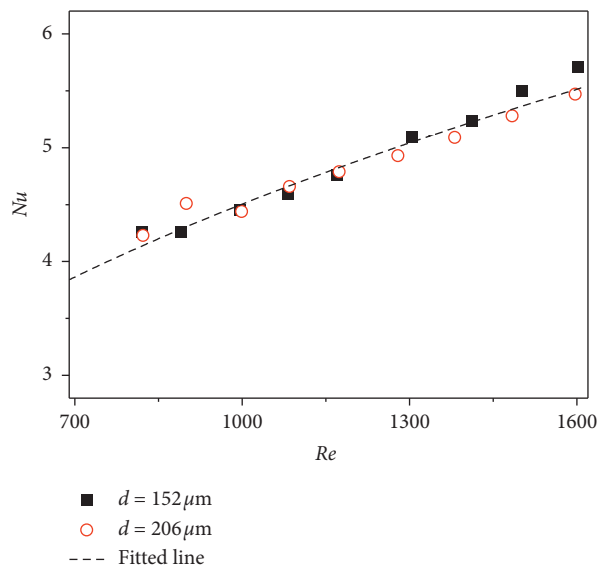FIGURE 9: Wall temperature of microchannels (liquid inlet temperature of 25°C).

FIGURE 10: Effect of the Reynolds number on the Nusselt number.

microchannel with a diameter of $152\,\mu$m under different flow and heat loads is depicted in Figure 9. The distribution of temperature on the wall of the microchannel is determined by the heat load and fluid flow rate, and the graph shows that the wall temperature increases approximately linearly along the wall. It is also seen that the wall temperature increases with the increase of heat flux at the same liquid inlet flow rate.

The change in the Nusselt number of liquid convection heat transfer in rough stainless microchannels with diameters of $152\,\mu$m and $206\,\mu$m with the Reynolds number is listed in Figure 10. The figure shows that the Nusselt number of laminar flow and heat transfer in rough microchannels is not only dependent on the shape of the cross section but also on the Reynolds number of liquid flow. It is observed in the

figure that the Nusselt number of liquid laminar convection heat transfer increases with increasing Reynolds number.

It is believed that the peaks of rough structures in microchannel reduce the flow area of the microchannel, resulting in an increase of the local velocity. Consequently, the local Nusselt number of the laminar flow heat transfer gets improved. More importantly, the convex and concave structures on the channel wall disturb the regular distribution of the thermal boundary layer. Together with the induced eddies near the microchannel wall surface, both then contribute to the increase of the local Nusselt number.

Similarly, a correlation equation of Nusselt number and Reynolds number is proposed for the prediction of laminar flow heat transfer in the circular roughness microchannel, and it is expressed as $\mathrm{Nu} = C_2 \varepsilon^{a_2} \mathrm{Re}^{b_2}$. The obtained correlation equation, with fitted parameters of $C_2 = 0.24$, $a_2 = 0.012$, and $b_2 = 0.431$, is also illustrated in Figure 10, presenting the acceptable agreement with experimental data.

4. Conclusions

In this study, a performance test system of heat transfer and liquid flow in rough microchannels was designed and built, and an experimental examination of heat transfer and liquid flow in rough microchannels was carried out, in which the three-dimensional morphology of the rough surface was observed by scanning electron microscopy. The Poiseuille number of liquid laminar flow and the Nusselt number of liquid laminar convection heat transfer in rough microchannels were obtained as a function of the Reynolds number. The major conclusions are drawn as follows:

(1) In rough microchannels, the Poiseuille number of liquid laminar flow relies not only on the shape of the cross section of the channel but also on the Reynolds number of liquid flow. The Poiseuille number of liquid laminar flow in rough microchannels increases with increasing Reynolds number, and the influence of roughness on liquid flow in rough microchannels gets much more obvious with the increase of the Reynolds number.

(2) In rough microchannels, the Nusselt number of liquid laminar flow heat transfer is related not only to the shape of the cross section of the channel but also to the Reynolds number of liquid flow, i.e., the Nusselt number raises with the increase of the Reynolds number.

Data Availability

The data used to support the findings of this study are available from the corresponding author upon request.

Conflicts of Interest

The authors declare that there are no conflicts of interest regarding the publication of this article.

Acknowledgments

References

[1] C.-M. Ho and Y.-C. Tai, "Micro-electro-mechanical-systems (MEMS) and fluid flows," *Annual Review of Fluid Mechanics*, vol. 30, no. 1, pp. 579–612, 1998.

[2] Y. Chen, W. Gao, C. Zhang, and Y. Zhao, "Three-dimensional splitting microfluidics," *Lab on a Chip*, vol. 16, no. 8, pp. 1332–1339, 2016.

[3] Z. Liu, M. Li, Y. Pang, L. Zhang, Y. Ren, and J. Wang, "Flow characteristics inside droplets moving in a curved micro-channel with rectangular section," *Physics of Fluids*, vol. 31, no. 2, Article ID 022004, 2019.

[4] S. R. Yadhuraj, S. Babu Gandla, S. S. Omprakash, B. G. Sudarshan, and S. C. Prasanna Kumar, "Design and development of micro-channel using PDMS for biomedical applications," *Materials Today: Proceedings*, vol. 5, no. 10, pp. 21392–21397, 2018.

[5] C. Zhang, Y. Chen, R. Wu, and M. Shi, "Flow boiling in constructal tree-shaped minichannel network," *International Journal of Heat and Mass Transfer*, vol. 54, no. 1–3, pp. 202–209, 2011.

[6] N. Ibrahim-Rassoul, E.-K. Si-Ahmed, A. Serir, A. Kessi, J. Legrand, and N. Djilali, "Investigation of two-phase flow in a hydrophobic fuel-cell micro-channel," *Energies*, vol. 12, no. 11, pp. 2061, 2019.

[7] C. Zhang, F. Yu, X. Li, and Y. Chen, "Gravity-capillary evaporation regimes in microgrooves," *AIChE Journal*, vol. 65, no. 3, pp. 1119–1125, 2019.

[8] J. Wang, W. Gao, H. Zhang, M. Zou, Y. Chen, and Y. Zhao, "Programmable wettability on photocontrolled graphene film," *Science Advances*, vol. 4, no. 9, Article ID eaat7392, 2018.

[9] J. B. Taylor, A. L. Carrano, and S. G. Kandlikar, "Characterization of the effect of surface roughness and texture on fluid flow-past, present, and future," *International Journal of Thermal Sciences*, vol. 45, no. 10, pp. 962–968, 2006.

[10] C. Zhang, Z. Deng, and Y. Chen, "Temperature jump at rough gas-solid interface in couette flow with a rough surface described by Cantor fractal," *International Journal of Heat and Mass Transfer*, vol. 70, pp. 322–329, 2014.

[11] X. Liu, Y. Chen, and M. Shi, "Dynamic performance analysis on start-up of closed-loop pulsating heat pipes (CLPHPs)," *International Journal of Thermal Sciences*, vol. 65, pp. 224–233, 2013.

[12] D. B. Tuckerman and R. F. W. Pease, "High-performance heat sinking for VLSI," *IEEE Electron Device Letters*, vol. 2, no. 5, pp. 126–129, 1981.

[13] S. Kandlikar, "Heat transfer, pressure drop and flow patterns during flow boiling in parallel channel compact heat exchangers of small hydraulic diameters," *Heat Transfer Engineering*, vol. 23, no. 5, pp. 5–23, 2001.

[14] Z. Li, W.-Q. Tao, and Y.-L. He, "A numerical study of laminar convective heat transfer in microchannel with non-circular cross-section," in *Proceedings of the ASME 3rd International Conference on Microchannels and Minichannels*, pp. 351–360, American Society of Mechanical Engineers (ASME), Toronto, Canada, June 2005.

[15] Z. Deng, X. Liu, C. Zhang, Y. Huang, and Y. Chen, "Melting behaviors of PCM in porous metal foam characterized by fractal geometry," *International Journal of Heat and Mass Transfer*, vol. 113, pp. 1031–1042, 2017.

[16] C. Zhang, Y. Chen, M. Shi, Y. Huang, and Y. Chen, "Effects of roughness elements on laminar flow and heat transfer in microchannels," *Chemical Engineering and Processing: Process Intensification*, vol. 49, no. 11, pp. 1188–1192, 2010.

[17] Y. Chen, C. Zhang, M. Shi, and Y. Yang, "Thermal and hydrodynamic characteristics of constructal tree-shaped minichannel heat sink," *AIChE Journal*, vol. 56, no. 8, pp. 2018–2029, 2010.

[18] K. D. Cole and B. Çetin, "The effect of axial conduction on heat transfer in a liquid microchannel flow," *International Journal of Heat and Mass Transfer*, vol. 54, no. 11-12, pp. 2542–2549, 2011.

[19] S. G. Kandlikar, D. Schmitt, A. L. Carrano, and J. B. Taylor, "Characterization of surface roughness effects on pressure drop in single-phase flow in minichannels," *Physics of Fluids*, vol. 17, no. 10, p. 100606, 2005.

[20] S. G. Kandlikar, S. Joshi, and S. Tian, "Effect of surface roughness on heat transfer and fluid flow characteristics at low reynolds numbers in small diameter tubes," *Heat Transfer Engineering*, vol. 24, no. 3, pp. 4–16, 2003.

[21] S. Shen, J. Xu, J. Zhou, and Y. Chen, "Flow and heat transfer in microchannels with rough wall surface," *Energy Conversion and Management*, vol. 47, no. 11-12, pp. 1311–1325, 2006.

[22] R. Shah and A. London, "Laminar flow forced convection in ducts," in *Advances in Heat Transfer*, Academic Press, New York, NY, USA, 1978.

[23] J. Stoer and R. Bulirsch, *Introduction to Numerical Analysis*, Springer Science & Business Media, Berlin, Germany, 2013.

[24] J. P. Holman, *Heat Transfer*, McGraw-Hill Education, New York, NY, USA, 10th edition, 2010.

[25] F. M. White, *Fluid Mechanics*, McGraw-Hill Education, New York, NY, USA, 8th ed edition, 2016.

[26] H. Y. Wu and P. Cheng, "An experimental study of convective heat transfer in silicon microchannels with different surface conditions," *International Journal of Heat and Mass Transfer*, vol. 46, no. 14, pp. 2547–2556, 2003.